Importance of FTIR Spectra Deconvolution for the Analysis of Amorphous Calcium Phosphates

Agnese Brangule[1,2], Karlis Agris Gross[1]
[1]Institute of Biomaterials and Biomechanics, Riga Technical University, P.Valdena 3, LV-1048,
[2]Riga, Latvia Riga Stradiņš University, Dzirciema 16, LV-1007, Riga, Latvia.

Keywords: amorphous calcium phosphate, bone, spectroscopy, FTIR-DRIFT, deconvolution

Abstract.
This work will consider Fourier transform infrared spectroscopy – diffuse reflectance infrared reflection (FTIR-DRIFT) for collecting the spectra and deconvolution to identify changes in bonding as a means of more powerful detection. Spectra were recorded from amorphous calcium phosphate synthesized by wet precipitation, and from bone. FTIR-DRIFT was used to study the chemical environments of PO_4, CO_3 and amide. Deconvolution of spectra separated overlapping bands in the υ_4PO_4, υ_2CO_3, υ_3CO_3 and amide region allowing a more detailed analysis of changes at the atomic level. Amorphous calcium phosphate dried at 80 ^oC, despite showing an X-ray diffraction amorphous structure, displayed carbonate in positions resembling a carbonated hydroxyapatite. Additional peaks were designated as A1 type, A2 type or B type. Deconvolution allowed the separation of CO_3 positions in bone from amide peaks. FTIR-DRIFT spectrometry in combination with deconvolution offers an advanced tool for qualitative and quantitative determination of CO_3, PO_4 and HPO_4 and shows promise to measure the degree of order.

Introduction

Amorphous calcium phosphate (ACP) plays an important role in the formation of biomaterials [1]. The diversity of possible arrangements within the apatite structure requires sensitive tools to detect changes from different synthesis conditions, especially for amorphous structures, that are even more difficult to characterize. Fourier transform infrared (FTIR) spectroscopy offers a method for monitoring changes in the chemical groups. This work will show how FTIR-DRIFT spectroscopy provides a simple, non-destructive technique to obtain yet unexplored information about amorphous calcium phosphates.

The aim of this study was to apply curve fitting deconvolution for investigating overlapping bands in the υ_4PO_4, υ_2CO_3, υ_3CO_3 band region in synthesized amorphous calcium phosphates and υ_3CO_3 and amide band in natural human bone. Deconvolution is based on J.K. Kaupinens et. al. methodology introduced in the 1980's [2] – a mathematical procedure for resolving overlapped peaks in a complex FTIR spectrum, also referred to as "resolution enhancement" without changes to the experimental spectral resolution [3].

The vibration band υ_4PO_4 was chosen in this study due to the υ_4PO_4 562 cm^{-1}, 575 cm^{-1} and 603 cm^{-1} peak overlap with the HPO_4 apatitic peak at 550 cm^{-1} [4]. Chemical determination of HPO_4^{2-} ions by colorimetry cannot be distinguished from PO_4^{3-}. Another method by Gee and Dietz [5] that condenses HPO_4^{2-} ions into pyrophosphates $P_2O_4^{4-}$ cannot be used for powders containing carbonate CO_3^{2-} ions. Carbonate ions interfere with $P_2O_4^{4-}$ ions and partially prevent $P_2O_4^{4-}$ ion formation [6]. Consequently, this spectral method is thus the only viable technique for determining the HPO_4^{2-} content in carbonated ACP.

Carbonate ion concentration can be determined by heating ACP to 1200 ^{o}C to liberate CO_2 for collection in an absorption cell. Carbonates can then be determined by calorimetric titration [7]. This analysis method only gives information on the quantity of carbonates. Deconvolution of υ_2CO_3 and υ_3CO_3 bands in FTIR spectra gives information about the apatite structure. Le Geros observed and interpreted IR peak splitting for the CO_3 to represent A and B type carbonate substitution models – representing OH and PO_4 replacement respectively [8]. Some researchers also reported A1 type, A2 type and B type substitution doublets [9-11] or A-B type apatites, and "nonapatitic" or "labile" CO_3^{2-}, PO_4^{3-} and HPO_4^{2-} [12,13].

Human bone consists mainly of collagen fibers and inorganic compounds, which can be approximated as carbonate containing hydroxylapatite [14,15]. Deconvolution of FTIR spectra will be shown to give information about overlapped amide I, amide II and amide III peaks in collagen, and inorganic υ_3CO_3 bands in the 900 – 1900 cm^{-1} region [15].

Materials and Methods

Materials

Three different carbonate containing ACPs were synthesized at room temperature and dried for FTIR analysis. The first two powders were prepared by mixing a solution containing $Ca(NO_3)_2$ and 30 % ammonia with another solution consisting of $(NH_4)_2HPO_4$ and $(NH_4)_2CO_3$. Drying of these first two wet powders was conducted in air at 20 ^{o}C for 72h, or in a convection oven at 80 ^{o}C for 24h. The third ACP was a Zn enriched ACP was prepared by mixing the solution ($Ca(NO_3)_2$, $Zn(NO_3)_2$ and 30 % ammonia) with $(NH_4)_2HPO_4$ and $(NH_4)_2CO_3$ solution followed by freeze-drying at -50 ^{o}C for 48 h.
Bone was sourced from human vertebra - stored at room temperature in air for 40 years.

Methods

Fourier transform infrared spectroscopy *– diffuse reflectance infrared reflection.* The functional group changes were determined by FTIR–DRIFT (PerkinElmer Spectrum One,) at 450–4000 cm^{-1}, at a resolution of 4 cm^{-1}, with an average of 8 scans, sampled by diamond sampling sticks. A special preparation method was not required for synthesized powders. Powder for bone analysis was obtained from the inside of bone vertebra.

Table 1. Domains, assignments and literature for nanocrystalline apatite

Domain, Assignments	IR (cm^{-1})	Reference
HPO_4 apatitic	551	12
υ_4PO_4	562, 575 and 603	12
PO_4 non-apatitic	617	12
non-apatitic	866	12
υ_2CO_3 type B	871	12
υ_2CO_3 type A	880	12
υ_2CO_3 type B	1460-1470	12
υ_2CO_3 type B doublet	~1455 and ~1410	11
non-apatitic	1500	12
type A	1540	12
υ_2CO_3 type A1 doublet	~1540 and ~1455	11
υ_2CO_3 type A2 doublet	~1565 and ~1505	11
B + non-apatitic	1420	12
Amide I	~1660 – 1690	15
Amide II	~1500 – 1600	15
Amide III	~1242	15

X-ray powder diffraction (XRD). Powders were characterized by X-ray diffraction (Bruker D8 ADVANCE diffractometer). Diffraction patterns were recorded from 5° to 60° using Cu K radiation (λ = 1.54 Å generated at 40 mA and 40 kV) at a step size of 0.2°. Analysis. The FTIR spectra were viewed and smoothed with freeware software Specwin32. Baseline correction and curve-fitting analysis was performed using MagicPlotStudent software with wavenumbers from literature as a guide for υ4PO4, υ2CO3, υ3CO3, amide I, amide II, amide III groups (Table 1). Deconvolution involved both Lorentzian and Gaussian curve fitting.

Results and Discussions

All synthesized ACPs displayed an X-ray amorphous structure - a broad low intensity peak centred at 30°, Fig 1. All three patterns appear similar.

FTIR-DRIFT spectra of three ACPs are shown in Fig 2. Phosphate bands (υ_1, υ_2 and υ_4PO_4) and carbonate bands (υ_2, υ_3CO_3) were detected. By using information from the literature (Table 1) we can infer that PO_4 bands overlap HPO_4 bands. Only small shifts in the IR spectra suggest a change in the chemical group placement.

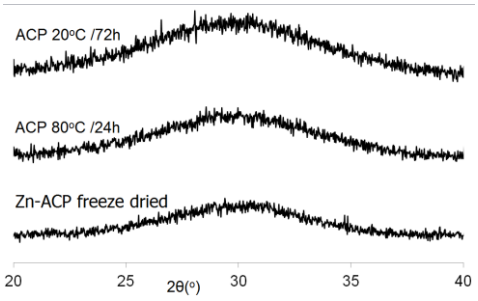

Fig 1. XRD patterns of air dried ACP, 80 °C dried ACP, freeze-dried Zn-ACP.

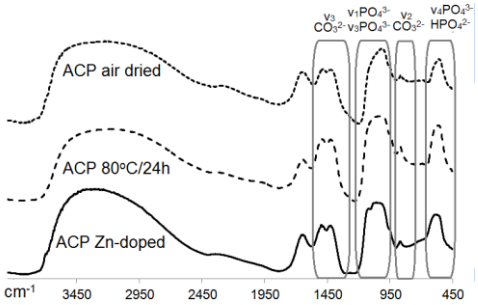

Fig 2. FTIR-DRIFT spectra of air dried ACP, 80 °C dried ACP, and freeze-dried Zn-ACP

Deconvolution of the 500-700 cm^{-1} region of all three FTIR spectra revealed the presence of HPO_4^{2-} (550 cm^{-1}) only in Zn-doped ACP (Fig 3).

Spectra obtained in the υ_2CO_3 band region (800 – 920 cm^{-1}) show a considerable change in peak shape and position. A shoulder at ~880 cm^{-1} was observed for the 80 °C dried powder, that was not present for the air dried powder. Using peak assignments from the literature, we can infer the presence of an A type substituted carbonate group. More detailed information on the structure of apatites can be obtained after deconvolution of the spectra. Deconvolution of the 800 – 920 cm^{-1} region displays only non-apatitic carbonate in air-

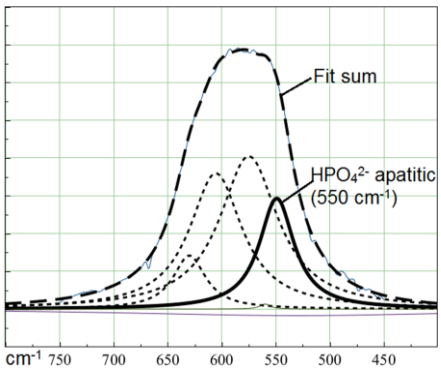

Fig 3. Deconvolution of Zn doped ACP showing $\upsilon_4PO_4^{3-}$ and HPO_4^{2-} band (450—700 cm^{-1})

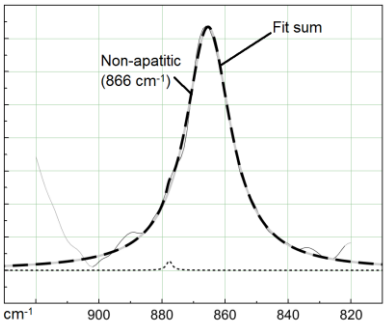

a

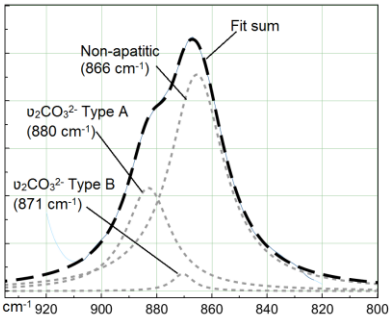

b

Fig 4. Deconvolution of band (800—920 cm^{-1}) showing the $\upsilon_2CO_3^{2-}$ in a) air dried ACP and b) 80°C dried ACP

dried ACP but additional A-type and B-type carbonate for 80 ^{o}C dried powders (Fig 4a and b). The carbonate type can be changed by drying at different conditions [16]. Air-dried powder mainly contained non-apatitic CO_3^{2-}, but drying at 80 ^{o}C produced more A-type and B-type carbonates as shown by peaks at 880 cm^{-1} and 871 cm^{-1}, respectively.

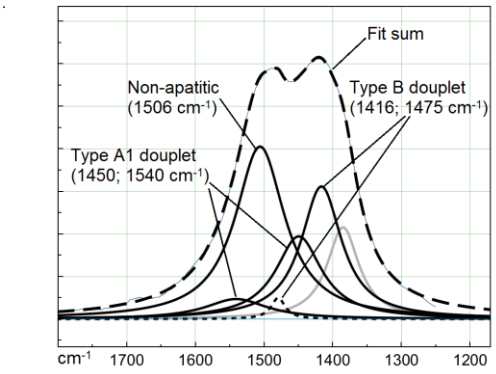

Fig 5. Deconvolution of $\upsilon_3CO_3^{2-}$ band (1200—1800 cm^{-1}) for 80 ^{o}C dried ACP

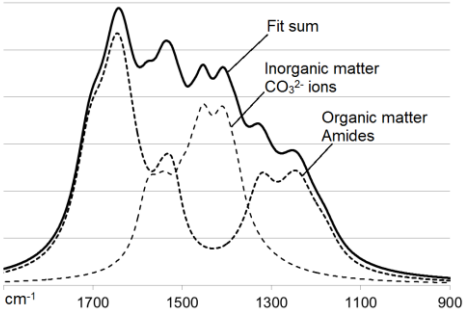

Fig 6. Deconvolution of human bone showing convoluted organic amide and inorganic carbonate bands (900 —1900 cm^{-1})

Additional information on carbonates powders can be sourced from the υ_3CO_3 (1400 - 1600 cm^{-1}) region. Higher crystallinity in relation to carbonates is interpreted by more carbonate occupying the A-type or B-type positions, characteristic of crystalline apatite. Poorly crystalline powder displayed an A 2 carbonate peak (at 1506 cm^{-1}) overlapping a non-apatitic CO_3^{2-} (at ~1500 cm^{-1}), Fig 5. The CO_3^{2-} is not easily determined, but the different CO_3^{2-} positions becomes clear from the numerous peak positions.

The most benefit from deconvoluting FTIR spectra is gained for human bone, Fig 6. The 1000 – 1900 cm^{-1} region has an overlap of amide and CH_2 peaks with carbonate peaks. Deconvolution of the FTIR spectra show convoluted organic amide bands, Fig 7. and inorganic carbonate υ_3CO_3 bands, Fig 8. Deconvolution of the organic band shows that Amide I, Amide II and Amide III bands dominate in this region. Deconvolution of the inorganic υ_3CO_3 bands shows a type A1 doublet, a type A2 doublet and a type-B doublet in this region. Two further peaks were added so that the fit sum peak corresponds to the recorded peak. A type-A2 substituted carbonate can be identified from the broad shoulder at ~1565 cm^{-1}.

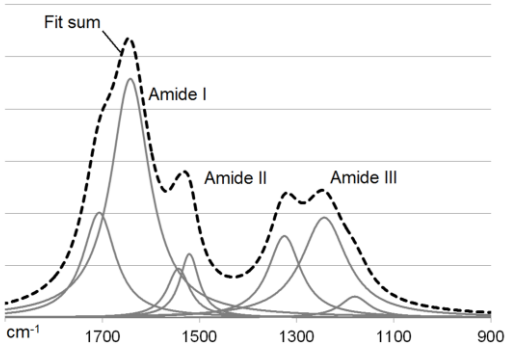

Fig 7. Deconvolution of human bone showing deconvoluted and convoluted amide band

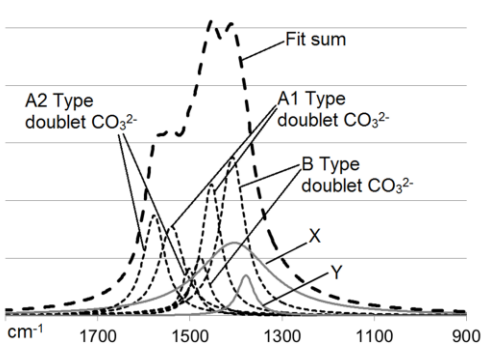

Fig 8. Deconvolution of human bone showing deconvoluted and convoluted carbonate band

Conclusions

Deconvolution of FTIR spectra offers a more detailed qualitative and quantitative analysis of carbonate ("non-apatitic" vs "apatitic") and orthophosphates (HPO_4^{2-} and PO_4^{3-}). The carbonate band (1400 - 1600 cm^{-1}) for the air dried powder shows non-apatitic positions, but drying at 80 ^oC showed peaks that coincided with crystalline carbonated apatite.

FTIR-DRIFT provides a sensitive, non-destructive tool for the analysis of bone, and with deconvolution can distinguish the inorganic carbonate bands from the organic amide bands.

Deconvolution of ACP spectra provides a new ability that may be used to track the transition of the amorphous phase to a crystalline apatite in bones as well as providing a tool to establish the influence of processing and drying conditions on the state of the amorphous calcium phosphate. The change in the bonding marks the first change from an amorphous to a crystalline state and so this tool will be able to bridge the gap in understanding between the amorphous state and nanocrystalline states.

Acknowledgements. A special thanks to M. Pilmane from the Riga Stradins University of Latvia, for providing the vertebra bone for FTIR analysis.

References

[1] LeGeros R Z In Brown P W 1994 Constantz B (Eds.) Hydroxyapatite and Related Materials 3-28
[2] Kauppinen J K *et al* 1981 *Appl. Spectrosc.* **35** 271–76
[3] Barth A Harris P 2009 Infrared spectroscopy – Past and Present. In: Biological and Biomedical Infrared Spectroscopy 1–52
[4] Rey C 1990 *et al Calcif. Tissue Int.* **46** 384-94
[5] Gee A Dietz V R 1953 *Ann. Chem.* **25** 1320-1324
[6] Elliott J C 1994 Structure and Chemistry of the Apatites and Other Calcium Phosphates
[7] Markovic M *et al* 2004 *J. Res. Natl. Inst. Stand. Technol*. **109** 553-568
[8] LeGeros R Z *et al* 1969 **25** 5-7
[9] Elliott J C *et al* 2002 *Adv. X-Ray Anal*. **45** 172-181
[10] Wopenka B Pasteris J D 2005 *Materials Science and Engineering*: *C* **25** 131–143
[11] Fleet M E *et al* 2004 *Am. Mineral.* **89** 1422-1432
[12] Eichert D *et al* 2007 J.B. Kendall (Eds.), Nova Science Publishers 93-145
[13] Rey C *et al* 1989 *Calcif. Tissue Int.* **21** 267-273
[14] Farre B *et al* 2014 *J. Afr. Earth Sci.* **92** 1-13
[15] Figueiredo M M *et al* 2013 *J. Struct Biol* **181** 207–222 doi:10.1016/j.jsb.2012.12.005.
[16] Brangule A Gross K A 2015 *Key Eng. Mat.* **631** 99-103, doi:10.4028/www.scientific.net/KEM.631.99